CHAPTER 5

MULTI-STAGE-MULTI-OBJECTIVE VOLT/VAR CONTROL AND OPTIMIZATION

5.1 Introduction

Widespread installations of DERs in low and medium distribution systems have enhanced the energy efficiency of the system and also helped to maximize the CVR utilization. However, large number of installations of DERs also resulting in some operational and control issues such as under/over voltage, reversible power flow, etc. Though, the centralized VVO can solve these issues to some extent but suffers from its adoption when sudden changes in the network behavior and lacks proper coordination during the intermittent behavior of PVs output. To resolve this issue, the authors of [19], [21], [77], [88], [91] have proposed PV smart inverter-driven control scheme to achieve a faster response of VVC. Besides, the VAR support through PV inverter using two-time scale VVC scheme has been introduced in [19]. The multi time-scaled CVR deployments using linear least square method has also been suggested in [20] incorporating PV inverter impact. However, this scheme needs efficient reactive power dispatch methodology in different timescales. Though in [19], [20] such schemes have been suggested, but the effect of system and inverter losses has not been addressed. Moreover, these issues are a matter of concern from the economic point of view as well.

On the other side, implementation of CVR does not guaranty the reduction in system losses, which may depend upon several other factors such as network topology, load models, and load types. Therefore, this chapter introduces a multi-objective VVO formulation operating in a multi time scale in the presence of multiple PV power plants.

Besides, multi-objective centralized VVO along with smart inverter-based local control algorithm has been proposed to address these issues during sudden changes and limited voltage reduction issues. The contribution of this chapter includes :i) A Multi-Stage Multi-Objective VVC (MSMO-VVC) algorithm for slow and fast time scale using Discrete Multi-objective PSO (DOMPSO) and droop characteristics scheme; ii) Demonstration of algorithm in the presence of PV system with different levels of penetrations and voltage reduction in distribution network; iii) Analysis of intermittent behavior of PV system output, application of PV inverter for faster response and effect of inverter losses; iv) Assessment of the proposed method in respect of technical and economic aspects.

5.2 MSMO-VVC Strategy

In this investigation, a multi-stage, multi-objective VVC strategy for smart grid-enabled CVR operation coordinated with multiple VVC devices in centralized as well local domain has been presented. The proposed MSMO-VVC aims to enable the CVR operation and meanwhile retaining the voltage profile within allowable range under uncertain behavior of PV power generation and variations in load demand profile. A closed-loop framework for smart grid-enabled CVR has been illustrated in Figure 5.1. It is the combination of VVO processor and CVR server assisted through ADMS. The ADMS is fed back by advance metering infrastructure, which updates the field monitored measurements at regular intervals. The fundamental task of VVO processor is to optimize the settings of VVC devices according to CVR server. The range of CVR duration and CVR voltage are set by control center operator in CVR server block according to requirement. Stage wise description of proposed control strategy has been delineated as under:

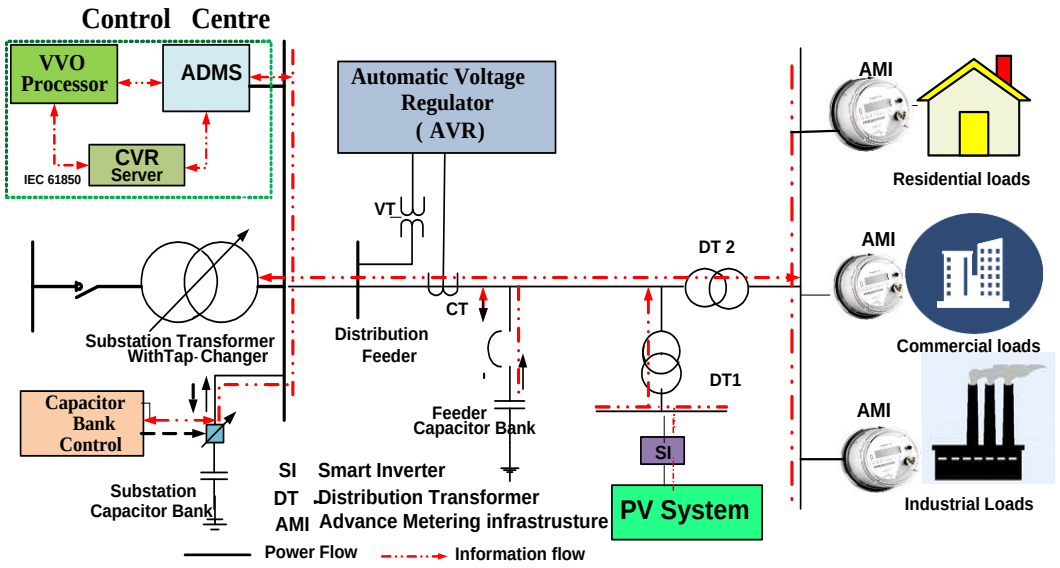

Figure 5.1 Proposed Substation Based closed-loop CVR

5.2.1 First Stage: Slow Time Scale Control (STSC)

In this stage, the actions of Volt/VAR regulating devices are optimized over a finite period with the coordination of central controller located at the substation control center. Therefore, this control is alternatively referred as a centralized control scheme. The control center operator fixed the CVR voltage level and sends control signals to the field devices.

The operation of this stage has been performed in two steps. Firstly, the expected CVR voltage and CVR time duration have been set through the CVR server. In the second step, the control parameters of Volt/VAR regulating devices have been optimized through VVO processor with the objectives of minimization of node voltage deviation from expected CVR voltage and system losses. ADMS regularly monitors and evaluates the power and voltage profile throughout the distribution network with the help of AMI.

5.2.2 Second Stage: Fast Time Scale Control (FTSC)

In the slow time scale stage, optimization of parameters of Volt/VAR regulating devices is carried out for a defined time horizon. However, during this time span (set in the first

stage), the deviation in PV active power with respect to forecasted value can be observed due to unexpected situations such as transient cloud movements, solar eclipse, etc. Consequently, it may cause violation of voltage limits. Therefore, the main objective of second stage is to maintain the voltage profile limits during the reduction of PV power output. The provision of decentralized or local domain-based additional reactive power compensation through fast time-scale control of inverter system has been suggested to fulfill.

A scheme using droop control-based principle has been employed to determine the compensating amount of reactive power from PV inverter such that VAR value is sufficient to achieve the desired voltage. In case, the PV output turns back to the forecast value or minimum allowable voltage is within limits, then the inverter output is retained to the optimal value as in the first stage.

5.2.3 Third Stage: Assessment of Proposed Control Method

The objective of third stage is to assess the employed CVR scheme in terms of amount of peak power reduction, energy, cost savings and CVR factors. In order to check the effectiveness of CVR in technical terms, CVR factor has been calculated in terms of peak kW power (CVR_{fP}) and kWh energy (CVR_{fE}). In the economic point of view, CVR factor has been calculated in terms of cost savings in purchased power. The detailed explanations have been already reported in *chapter 4* subsection 4.2.2 using equations (4.1) – (4.9).

5.3 Problem Formulation and Solution

The main objective of the present investigation is to achieve maximum energy demand reduction and peak shaving in a distribution network through CVR without violating the service voltage profile considering the transient behavior of PV power output. In order to

achieve this, the control scheme for CVR implementation has been formulated in two different time scale slow and fast as delineated under:

5.3.1 Optimal Control Action Under Slow Time Scale

Under the slow time scale control of CVR, the optimal settings of various controllers (OLTC/AVRs taps, steps of Q_{CBs} and Q_{PV} inverters) at the desired time have been determined. Mainly, the CVR is implemented by minimizing the node voltage deviation from expected CVR voltage without negotiating with the system regulatory standards. However, it has been observed that while applying CVR in order to reduce the voltage, increase in losses takes place [51], [20] which is an economically undesirable feature. To overcome, the problem has been combined to form a multi-objective formulation consisting of minimization of the voltage deviation and system losses.

Generally, multi objective optimization problem for N objectives formulated by equation (5.1).

$$\text{minimize } f(\vec{x}) = [f_1(\vec{x}), f_2(\vec{x}), f_3(\vec{x}), ... f_N(\vec{x})] \tag{5.1}$$

satisfying m inequality and p equality constraints equations (5.2) and (5.3) respectively.

$$g_i(\vec{x}) \leq 0 \;\; i = 0,1,2,3.....m \tag{5.2}$$

$$h_i(\vec{x}) = 0 \;\; i = 0,1,2,3.....p \tag{5.3}$$

where $\vec{x} = [x_1, x_2, ...x_n]$ is the decision variables vector.

Multi-objective optimization provides a set of optimal solution vectors rather than a unique optimal solution. An optimal solution vector has two possibilities that any solution can dominate other or no one dominates the other solutions. The nondominated solution (NDS) vector in the search space is defined as pareto-optimal solutions. These pareto

optimal solution vector produces near-optimal trade-off fitness values, which are known as the Pareto front surfaces.

5.3.1.1 Multi-Objectives:

The above discussed two objectives can mathematically, in terms of system variables, be expressed as:

- *First Objective Function (f_1):* The first objective function (f_1) has been represented as the minimization of the sum of the square of the deviation of node voltages from the expected CVR voltage in all phases and all nodes except source node at each hour to maximize the energy saving.

$$f_1 = \min\left\{\sum_{a,b,c}\sum_{i}^{N-1}\left(V_{i,h}-V_{CVR,h}\right)_{a,b,c}^{2}\right\} \tag{5.4}$$

where, $V_{i,h}$ is the node voltage (p,u.) at i^{th} bus at hour, h and $V_{CVR,h}$ is the expected CVR voltage (p,u.) at hour, h and N is the number of the nodes with phase notations of *a,b,c* respectively.

- *Second Objective Function (f_2):* Minimization of total system losses for all phases at each hour is the second objective function, f_2, which can be expressed as:

$$f_2 = \min\left\{\sum_{a,b,c}\left(P_{a,b,c}^{loss,h}+Q_{a,b,c}^{loss,h}\right)\right\} \tag{5.5}$$

where, $P_{a,b,c}^{loss,h}$ is the active power losses at hour, h and $Q_{a,b,c}^{loss,h}$ is the reactive power losses at hour, h.

5.3.1.2 System Constraints:

- *Transformer/regulator tap constraints:* The tap range of OLTC transformers/AVR and tap position are given in equations (4.18) and (4.19) respectively.

- *Transformer edging constraints:* In order to prevent the degradation of the life cycle of transformers, the daily tap operation of OLTC/AVR is governed by (3.18). In this study the value of $N^{i}_{tr,max}$ is considered 10 per phase.
- *Capacitor bank constraints:* Reactive power supplied by i^{th} CB (Q^{i}_{CB}) is determined using equation (1.12) and detailed explained in chapter 1 and daily switching operation of CBs should follow the relation shown in equation (3.11).
- *Solar PV Inverter:* Modern PV inverters have the capability to inject or consume the reactive power from the grid and operate as distributed Volt/VAR control devices. The more details can be found in chapter 1 subsection *1.4.2.3*.

The reactive power supplied by k^{th} PV inverter during slow time scale period ($Q^{k}_{PVst,T}$) is determined using equation (5.6).

$$Q^{k}_{PVst,T} = N^{k}_{PV}\ \Delta Q^{k}_{PV} \tag{5.6}$$

where, $N^{k}_{PV} = \{0,1,2....,N^{k,\max}_{PV}\}$, ΔQ^{k}_{PV} and $N^{k,\max}_{PV}$ are the switching step number, variation in reactive power per step and available maximum number of switching steps at k^{th} PV system respectively. The value of $N^{k,\max}_{PV}$ is dependent on at $Q^{inv,max}_{T}$ each time interval T

- *Voltage constraints:* Minimum and maximum voltage (V_{min}, V_{max}) at i^{th} node should remain within limits as shown in equation (3.13).

5.3.1.3 Solution through discrete multi-objective PSO

A multi-objective PSO approach has been employed to solve the desired optimization problem.

- *Overview of PSO:* Eberhart and Kennedy[135] introduced a powerful search-based optimization algorithm inspired by social behavior metaphor known as Particle

Swarm Optimization. The algorithm is initialized with a population array of particles with random velocity and positions in problem space to find the optima. The movement of a particle' position is based on its previous position and current velocity. PSO dynamic employs two main terminologies i.e. personal best (pbest) and global best (gbest). The pbest value of each particle is the best position so far it has achieved and best value among all pbest is called as gbest. The value of gbest at final iteration is the solution of the optimization problem.

- *Multi-Objective PSO(MOPSO):* The multi-objective optimization problem represented by equations (5.4) - (5.5) followed by system constraints has been solved using MOPSO approach. The MOPSO uses the repository to archive the positions of the particles that present nondominated solutions (NDS) so far [136]. The previously archived NDS leads the convergence toward globally NDS solutions. The velocity ($V_m^{K_r}$) and position ($X_m^{K_r}$) of each particle at K_r^{th} iteration is updated by equations (5.7) and (5.8), respectively.

$$V_m^{K_r+1} = wV_m^{K_r} + c_1 r_1 (P_m^{best} - X_m^{K_r}) + c_2 r_2 (P_r^{rep} - X_m^{K_r}) \quad (5.7)$$

$$X_m^{K_r+1} = X_m^{K_r} + V_m^{K_r+1} \quad (5.8)$$

where, w is inertia weight, c_1, c_2 are personal and global learning coefficients, r_1, r_2 are random numbers ranging between 0 and 1, P_m^{best} is the best position of the m^{th} particle and P_r^{rep} is a repository value. The position and velocity of the particles are updated and the value of objective functions calculated repetitively until the desired stopping criteria is not met. Multi-objective optimization provides a set of optimal solution vectors rather than a unique optimal solution. The NDS vector in the search space are defined as Pareto-optimal solutions. These pareto optimal solution vector produces near-optimal trade-off

fitness values, which are known as the pareto front surfaces. In order to determine the single optimal solution vector from various points generated by pareto dominance solutions, a minimum radial distance from the origin has been calculated. To achieve this, the normalization of fitness value concept has been employed using the equation (5.9).

$$\text{norm}(f(z)) = \frac{f(z) - \min(f(z))}{\max(f(z)) - \min(f(z))} \quad z \in \text{optimal pareto solutions} \tag{5.9}$$

- *Discrete MOPSO (DMOPSO):* Since the control variables (tap positions and switching steps) of the present problem are a discrete integer in nature; the MOPSO solution variable needs to be discretized. In order to do so, the solution variables obtained by (5.5) $X_{md}^{K_r+1}$, in the dth dimension are round off to its nearest integer value using the bracket function as shown in equation (5.10) [136]:

$$x_{md}^{K_r+1} = [X_{md}^{K_r+1}],\ d:\ 1 \rightarrow n$$
$$X_{md}^{K_r+1} \in \Re \ \text{and}\ x_{md}^{K_r+1} \in Z. \tag{5.10}$$

5.3.2 Action Under FTSC using Modified Droop Controller

In fast time scale, VVC has been carried out PV inverters only. The voltage regulation executed through inverter-based VAR dispatch. In order to determine desired compensating VAR from PV system, the droop characteristics based scheme has been utilized for PV inverter VAR control. The Volt/VAR droop characteristics for present problem is shown in Figure 5.2. It is piecewise linear to the voltage and changes dynamically due to its dependency on the PV active power . The droop characteristics is obtained by defining the four points (P_1, P_2, P_3 and P_4) parameters.

Determination of droop characteristics parameters are essential requirements because the reactive power compensation from PV inverters heavily depend upon defined values of

droop points and dead band. The settings of droop parameters vary according to the task requirements. The local control operator has flexibility to choose the appropriate setting according to their needs. In the droop control method, the dead band (DB) range plays an important role. Generally, it is defined as the width between points P_2 and P_3 in which inverter neither absorbs nor injects the VAR. In DB range, the compensated reactive power is zero. However, the PV inverter still feeds the reactive power as defined in STSC. Before the point P_2, inverter can inject the additional reactive power to the grid till point P_1 is reached. After point P_1, inverter can inject the available maximum reactive power. However, when the voltage is above point P_3, inverter absorbs aditional reactive power from the grid till point P_4. After point P_4 is reached, inverter absorbs the available maximum reactive power. The compensated reactive power($\Delta Q_{com,t}^{inv}$) at any instant, t is determined using (5.11).

$$\Delta Q_{com,t}^{inv}(V) = \begin{cases} Q_t^{inv,max} & V < V_1^{P_1} \\ \dfrac{V - V_1^{P_1}}{V_1^{P_1} - V_2^{P_2}} Q_t^{inv,max} & V_1^{P_1} \le V < V_2^{P_2} \\ 0 & V_2^{P_2} \le V \le V_3^{P_3} \\ -\dfrac{V - V_3^{P_3}}{V_4^{P_4} - V_3^{P_3}} Q_t^{inv,max} & V_3^{P_3} < V \le V_4^{P_4} \\ -Q_t^{inv,max} & V > V_4^{P_4} \end{cases} \tag{5.11}$$

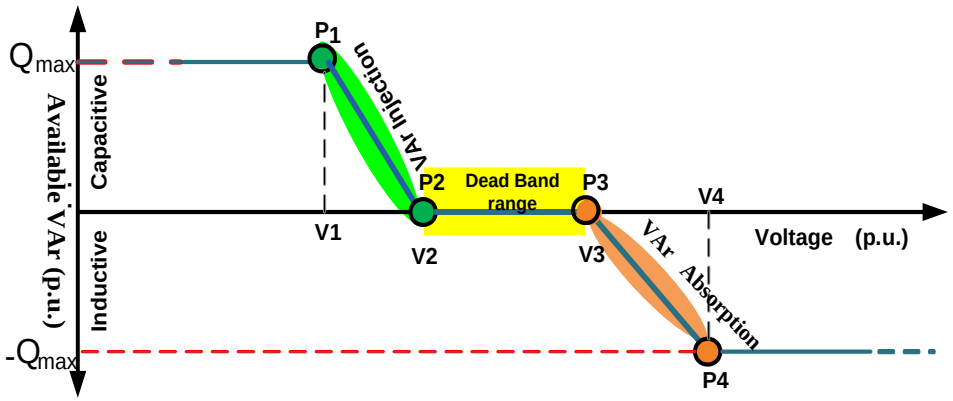

Figure 5.2 Volt/VAR droop characteristics

where, $Q_t^{inv,max}$ is the maximum VAR capacity of the inverter at instant, t, as defined in equation (1.16).

$$Q_{Total,t}^{inv} = Q_{PVst,T}^{k} \pm \Delta Q_{com,t}^{inv} \leq \left| Q_t^{inv,max} \right| \quad (5.12)$$

where $Q_{PVst,T}^{k}$ is the optimal VAR value during first stage.

5.4 Implementation of Proposed MSMO-VVC

Figure 5.3 shows the flowchart of the implementation of the proposed MSMO-VVC method with various stages, as described below.

The stepwise execution procedure of *First Stage* (STSC) has been described done in *algorithm 1* as under:

Algorithm 1 STSC Parameters optimization using DMOPSO	
1	**Input:** Feed the distribution network data {loads, lines, VVC devices and PV plant data (if PV present)}
2	**Input:** PSO parameters and control varriable limit
3	Set the expected CVR voltage and CVR time duration.
4	Divide the particle dimensions among control variables (as tap positions of OLTC, AVRs, and switching steps for CBs & PV inverters)
5	Set the stopping criteria (maximum number of iterations)
6	Initialize the population and speed of all the particles and perform load flow analysis.
7	Evaluate the value of fitness functions expressed using (5.4) and (5.5) for each particle.
8	Find P_{best} and G_{best} of the particles
9	Identify the positions of the particles that represent nondominated vectors and store in the (P^{rep}) repository.
10	Update velocity and position of each particle using (5.7) and (5.8), respectively.
11	Evaluate the position of the particles and update the P^{rep} repository.
12	Check the stopping criteria if yes then go to 13 else go to step 6.
13	Determine the single optimal solution vector using a minimum radial distance from the origin.
14	Prioritize the solution, further assigning the proper weightages to the objective functions.
15	**Output:** Adopt the VVC settings corresponding to top priority objective.

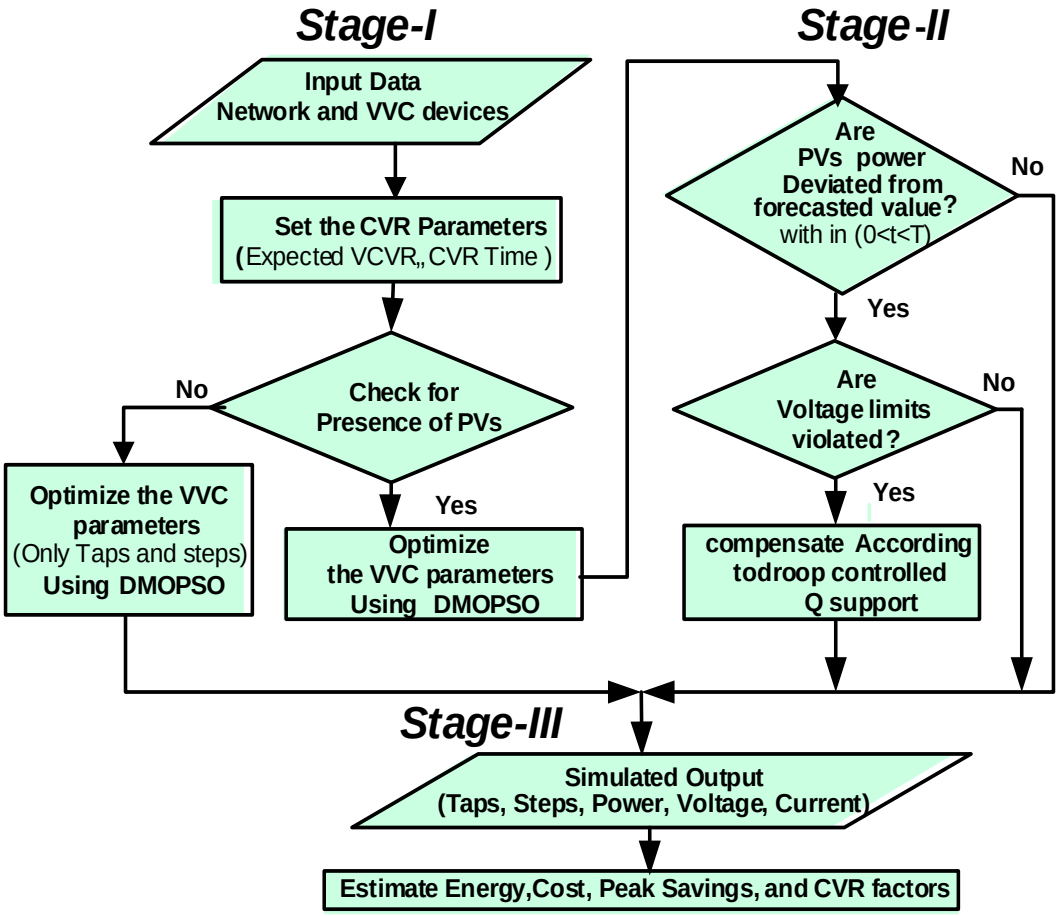

Figure 5.3 Flow chart of implementation of three stages of proposed method

The solution obtained from *Algorithm 1* can directly be implemented for CVR operation for first stage.

- In the *Second Stage* (FTSC) implementation, the DMOPSO solution include the reactive power compensations in case of voltage limit violation due to the deficit in PV system output. The droop control action solution obtained from algorithm 2 directly implemented in stage 2.
- The solutions obtained from *algorithms 1 and 2* can be directly utilized in the *Third Stage* for the estimation of the total active power demand reduction, ΔP_{demand}, energy savings, ΔE_{saving}, cost savings, ΔC_{saving} and CVR factors using equations (4.1) – (4.9). respectively.

Algorithm 2 Droop based controller for FTSC

Input: Feed the optimal VVC parameters for considered CVR duration obtained through Algorithm 1
Input: Feed the droop characterstics parameters (P_1, P_2, P_3 *and* P_4 and dead band)
for time duration 0< t < T (as defined in STSC)
If, PV power output deviates from forecasted value
Then check the voltage limits
Else if voltage profile is in dead band range (between point P2 and P3)
Control action: No action is required.
Else if *lower limit of voltage is violated*
Then droop controller operates in capacitive region (before point P2) as shown in Figure 5.2
Control action: Injects the compensated reactive power determines by equation (5.11) followed by equation (5.12)
Else if *upper limit of voltage is violated*
Then droop controller operates in inductive region (after point P4) as shown in Fig.2
Control action: Absorb the compensated reactive power determines by equation (5.11) followed by equation (5.12)
Else follow the same instruction as suggested by *Algorithm 1*
end
Output: Desired additional reactive power compensation has been achieved

5.5 Simulations and Validation

5.5.1 Test System

The proposed CVR control has been validated on the modified IEEE 123 node distribution test feeder with the composite ZIP load model as shown in Figure 5.4[114]. The values of ZIP coefficients can be found in Appendix A in Table A.2.The optimization and control strategies have been developed in MATLAB, while test system modeled and load flow analysis has been done in the OpenDSS platforms. The test system consists of one OLTC, three AVRs, four switched shunt CBs and three PV systems. The OLTC and AVR transformers have ±16 taps with a per step increment of 0.00625. The OLTC

substation transformer is connected between nodes 150-149. The other three distributed AVRs are connected between nodes 9-14(AVR-1), 25-26(AVR-2), 160-67(AVR-3) respectively. The three-phase CB (Cap-1) is connected to node 83, having 200 kVAR per phase capacity with step variations from 0 to 4. Three single-phase CBs (Cap-2, Cap-3and Cap-4) are connected to node 88_a, 90_b, and 92_c, respectively, having a maximum rating of 50 kVAR. The three PV systems are connected to nodes 65abc (PV_1) 26ac (PV_2), and 104c (PV_3) with the inverter ratings of 1000 kVA, 800 kVA and 400 kVA respectively. Per step, reactive power variation from PV inverter is 50 kVAR for slow time scale. Moreover, the total KVA load demand shared by phase a, b, c is 40.5%, 27% and 32.5% respectively. The hourly load demand and grid electricity price (Indian Energy Exchange–Northern Grid (N2)) for an entirely typical day has been taken from [134] and [137] as shown in Figure 5.5. The controlling parameter used in DMOPSO is depicted in Appendix B in Table B.1

.

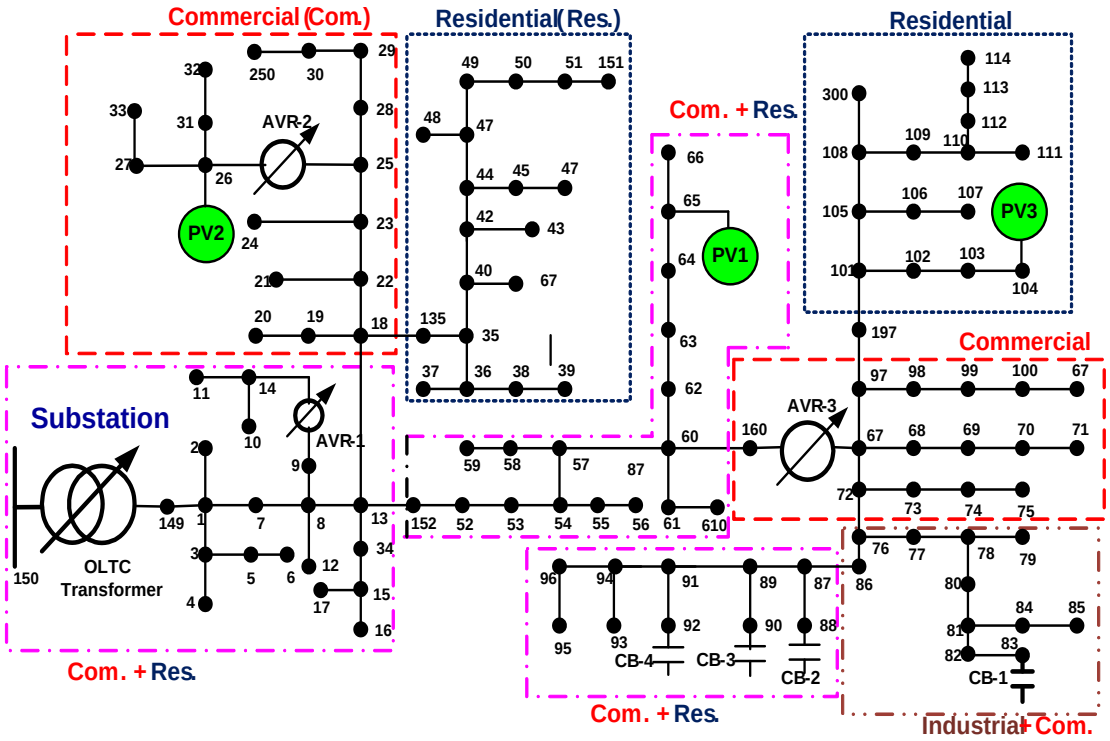

Figure 5.4 Modified IEEE 123 node distribution test feeder

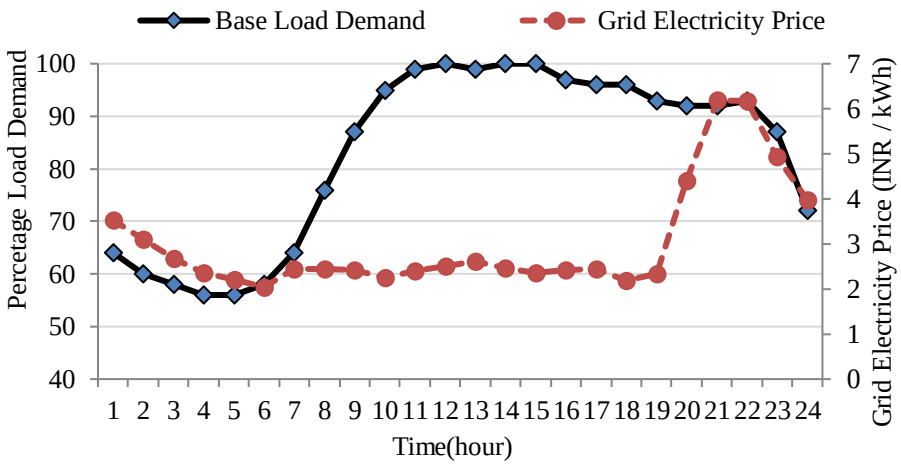

Figure 5.5 Hourly load demand and grid electricity price curve

5.5.2 VVC Modes of Operation

The performance of proposed method has been validated for two different time scale (slow and fast) under the following three different modes of VVC operation.

- *Mode 1: No-CVR (Base or Normal Operation):* In this mode, the system does not deploy CVR for VVC operation. The execution of VVC has been carried out with OLTC, AVR-1, AVR-2 at 120V regulated voltage and AVR-3 at 124 V. The fixed CBs have been used. Impact of PV power has not been considered.
- *Mode 2: Only CVR:* In this mode, the operation of VVC devices is carried out with proposed optimal CVR scheme using DMOPSO. The integration with PV system has not been considered in this mode of operation also.
- *Mode 3: CVR with PV:* In this mode, the proposed CVR scheme deploys with PV system also. The allocation of PV systems has been determined based on minimum node voltage.

5.5.3 Validation Under Slow Time Scale Control

The validation of the proposed method under STSC has been studied for two scenarios; peak shaving and daily energy-saving under the above-mentioned modes of VVC operation.

5.5.3.1 Scenario-I Peak Shaving

Peak shaving through CVR during a typical day has been studied in this scenario. The 14th hour of the daily load curve (as shown in Figure 5.5) is considered as a peak loading hour. The test system has been simulated for three modes of VVC operation at considered peak load hour.

- *Mode 1:* The simulation results of this mode are depicted in the second column of Table 5.1. Total active power demand and losses are 3619.2 kW and 96.7 kW respectively. Vmin and Vmax are 0.9787 and 1.0482 observed at nodes 65a and 83b respectively.
- *Mode 2:* The test system is simulated for only CVR with the proposed method. The NDS at $V_{CVR,h}$ of 0.95 p.u. at peak loading hour of 14th hour has been obtained. The pareto dominance front of these NDS are shown in Figure 5.6(a). In order to figure out the single set of decision variables from obtained NDS, a priority-based scheme has been used for decision making. A weightage of 70% has been assigned to the first objective function. The corresponding weightage factor is multiplied with the normalized fitness value of first objective function while calculating the distance from the origin. The simulated results of corresponding decision variables for this mode are depicted in the third column of Table 5.1. From the above results, it has further been observed that about 85 kW demand (2.35% peak power demand) has reduced with small reduction of 0.3% in system losses within the allowable voltage range. The effect of variation in expected CVR voltage (V_{CVR}) on kW peak demand reduction is shown in Figure 5.7 This figure illustrates that the percentage peak demand reduction increases with a reduction in CVR voltage within the expected range.
- *Mode 3:* In this mode, CVR is applied with PV power penetration in addition to earlier mentioned VVC devices. In order to choose the unique solution from NDS, the

procedure of Mode-2 has been adopted. The study of this mode is carried out for different levels of penetration under three cases. The pareto dominance fronts of these cases are shown in Figure 5.6 (b). The simulation results are depicted in fourth column of Table 5.1.

i) Case-I: CVR with 30% PV Penetrations (Single PV): CVR is deployed with 30% PV penetrations during peak load demand of 14^{th} hour of load duration curve shown in Figure 5.5. Active and reactive power injected by a three-phase PV1 source at node 65abc. Simulation results and other parameters such as PV power supplied, tap positions and CB steps are depicted in fourth column of Table 5.1. From the results, it can be observed that system active and reactive power losses reduced about 37.2% after and 42.9 % respectively. Total peak active power purchase from transmission grid has been reduced to 30%.

ii) Case-II: CVR with 50% PV Penetrations (Two PVs): In this case, CVR is applied along with 50% PV penetrations using three-phase PV1 and two-phase PV2 systems at 65abc and 26ac nodes. The total active & reactive power losses have been reduced to 46.1% and 53.45% respectively. Peak active power has reduced to 50.45 % without affecting customer devices.

iii)Case-III: CVR with 60% PV Penetrations (Three PVs): In this case, CVR is applied along with 60% PV penetrations using three-phase PV1, two-phase PV2 and single-phase PV3 systems at 65abc, 26ac and 104c respectively. The total active and reactive power losses have been reduced to 47.98% and 55.77% respectively. Peak active power has reduced to approx. 60 %. Though, during higher PV penetrations without incorporating

CVR affect results in overvoltage problem. However, this issue can be resolve deploying CVR at higher PV penetration levels.

The effect of different expected CVR voltage on KW peak demand reduction during PV penetrations with and without CVR is shown in Figure 5.8. This figure illustrates that peak shaving is higher in PV with CVR instead off only PV.

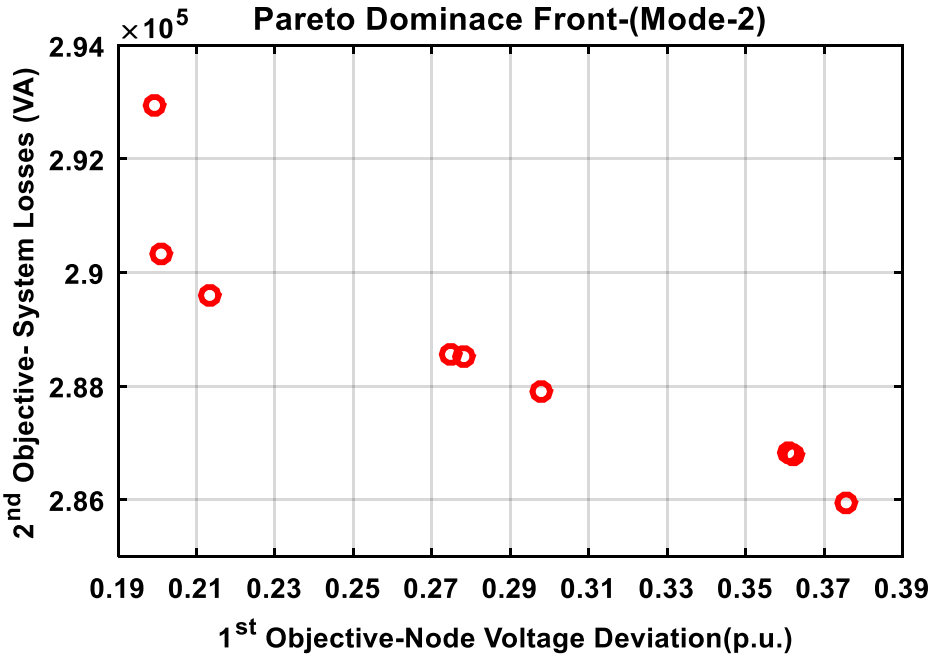

(a)

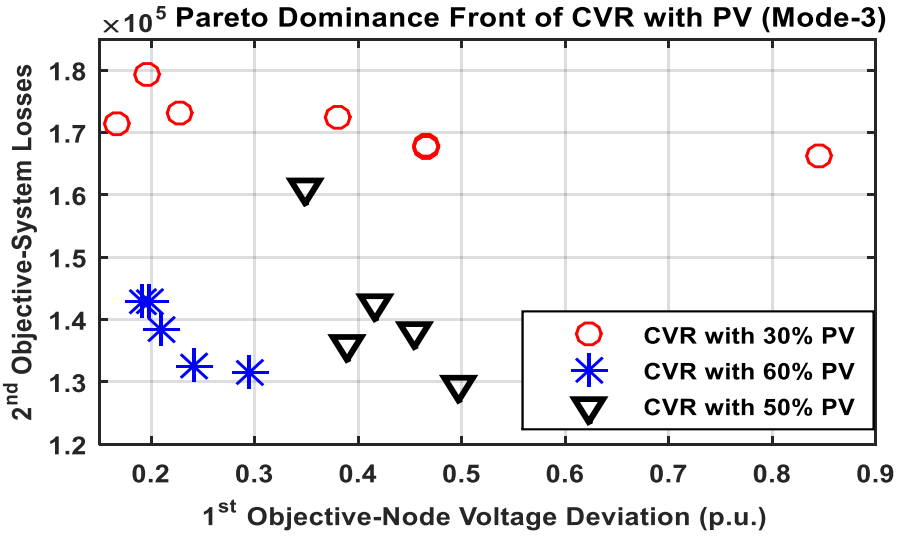

(b)

Figure 5.6 (a) Pareto dominance front for mode-2 (b) Pareto dominance front for CVR with PV

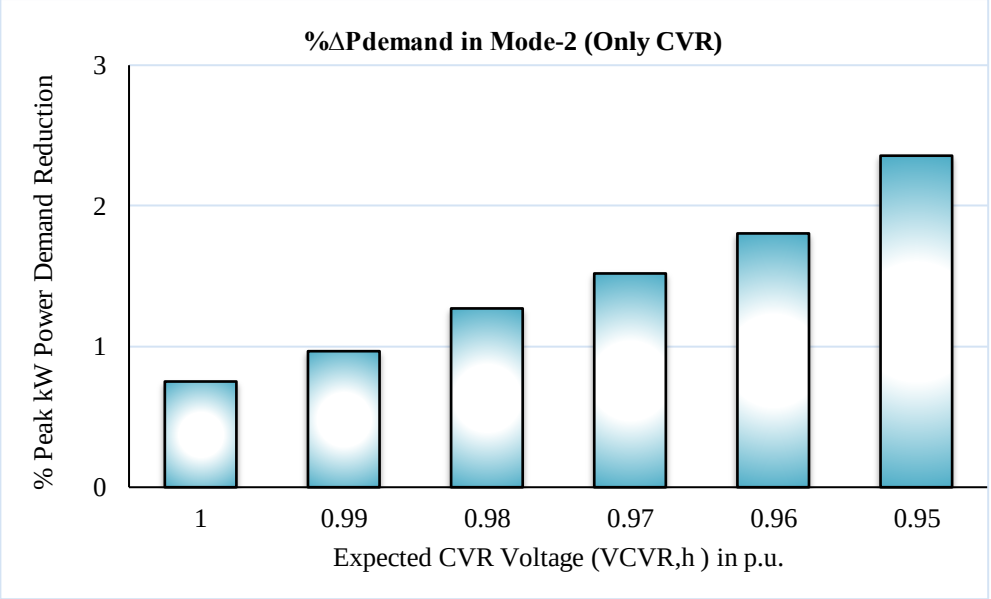

Figure 5.7 Active (kW) power demand reduction with different $\%V_{CVR}$ at peak load during Mode-2 operation

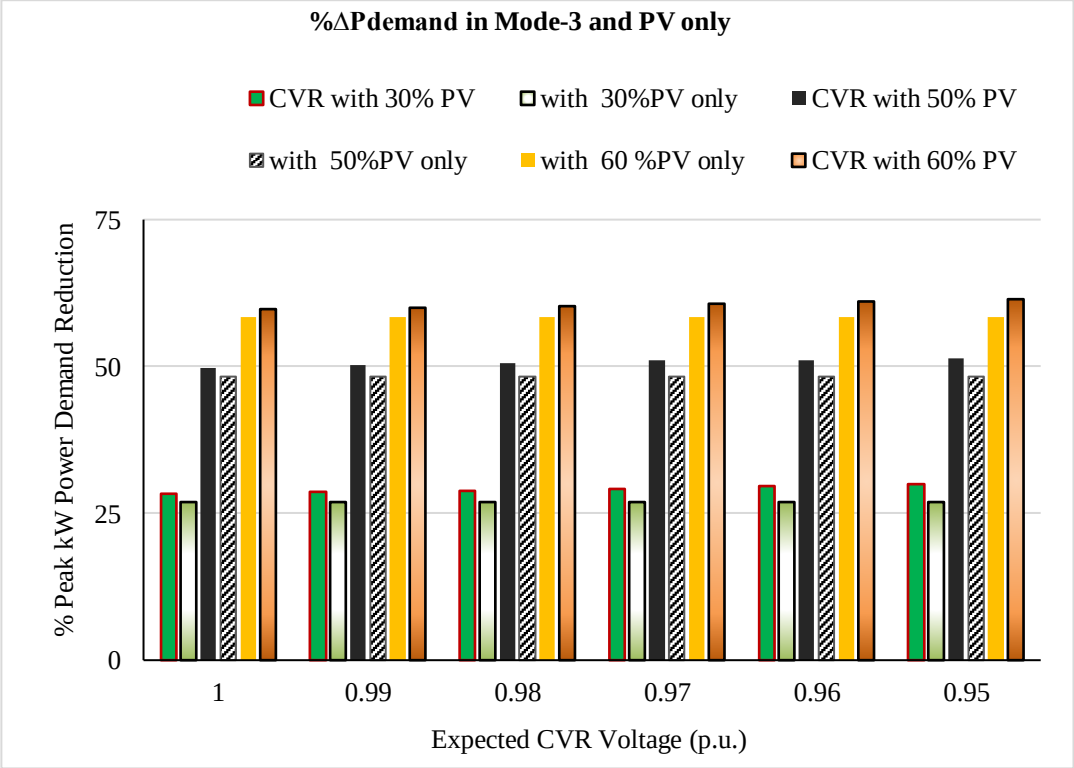

Figure 5.8 Active (kW) power demand reduction with different $\%V_{CVR}$ at peak load during Mode-3 operation and PV only

Table 5.1 Simulation Results of Scenario I

Parameters		**Mode-1 (No-CVR)**	**Mode-2 (CVR Only)**	**Mode -3 (CVR with PV Penetrations)**		
				30% PV	**50%PV**	**60% PV**
P_{demand} (kW)	**Φa**	1467.1	1434.1	1091.1	700.8	707
	Φb	962.5	941.2	615.9	614.6	613.2
	Φc	1189.6	1158.6	829.3	444.6	74.7
	Total	3619.2	2536.2	2536.2	1760.0	1395.0
ΔP_{demand} (kW)	**Φa**	---	33	376	733.3	727.1
	Φb	---	21.3	346.6	347.9	349.3
	Φc	----	31	360.3	745	1114.9
	Total %	----	85 (-2.35)	1082.9 (-29.9)	1826.2 (-50.45)	2119.3 (59.55)
Plosses, kW		96.7	96.46	60.7	50.6	50.3
Qlosses, kVAR		193.8	193.15	110.6	90.2	85.7
ΔPlosses, kW (%)		---	0.284 (-.3)	36 (-37.2)	46.1 (47.63)	46.4 (-47.98)
ΔQlosses, kVAR, (%)		------	-0.63 (-0.32)	83.2 (-42.9)	103.6 (53.45)	108.1 (-55.77)
P(kW), Q(kVAR) injected	**PV1**	--	----	960,200	960,100	960,200
	PV2	---		----	768,000	768,100
	PV3	----		----	---	368,100
Vmin (p.u), At node		0.9787 (65a)	0.9515 (32a)	0.9518 (114a)	0.9517 (114a)	0.9505 (114a)
Vmax (p.u), At node		1.0482 (83b)	1.0121 (150)	0.9994 (150)	1.0195 (150)	1.0334 (26)
Tap Position	**OLTC**	{+6}	{+2}	{0}	{0}	{0}
	AVR-1	{0}	{-3}	{0}	{0}	{0}
	AVR-2	{ +2, 0}	{1, -4}	{5, 4}	{ 5, 4}	{ 5, 4}
	AVR-3	{10,4,6}	{3,-4,2}	{1-2,1}	{1-2,1}	{1-2,1}

5.5.3.2 Scenario-II Daily Energy Savings

In order to reduce the daily energy demand, CVR has been employed for a typical whole day with and without PV penetrations through proposed CVR approach. Daily load demand and grid electricity price profile shown in Figure 5.5 has been considered. In order to demonstrate the effectiveness of the proposed method, the forecasted active power profile of PV systems has been assumed as shown in Figure 5.9. The simulation of the test system has been carried out in all three modes. The simulation results have been depicted in Table 5.2. It can be observed from this table that in Mode-2 operation the daily energy saving of about 1.5 MWh has been achieved with a 0.3 % reduction in energy losses. Thus about 2.1% of energy demand has been reduced without compromising system voltage profile. However, the energy losses it can further be reduced with the penetration of PV power.

CVR operation with different levels of penetration as 30%, 50%, and 60% have been carried out in mode-3 operation. Simulated results depicted in Table 5.2 shows that up to 18.65 to 28% and 21.22 to 31.5% reduction in active (ΔE^{P}_{losses}) and reactive (ΔE^{Q}_{losses},) energy losses respectively have been obtained with various levels of PV penetrations. The optimal reactive power injection has been provided from PV inverters when load demand is above 60% of peak load when higher losses take place. The impact of PV inverter losses has also been considered while calculating total losses. Figure 5.10 shows the optimal reactive power support from PV systems at various levels of penetrations. In case 60% PV penetration is applied without CVR operation, an undesirable event of rise in voltage above the upper threshold (1.054 p.u. at 12:00th hour) has been observed. However, when high-level PV penetration is carried out with CVR, the maximum node voltage has been found to be 1.033 p.u., which is within the permissible range. Even then there is a scope of further increase in PV penetration level

until maximum node voltage up to upper threshold of 1.05 p.u. is observed. Figure 5.11 shows the daily OLTC tap positions.

Table-5.2 Simulation Results of Scenario II

Energy Terms	**Mode-1 (No-CVR)**	**Mode-2 (CVR only)**	**Mode-3 (CVR with PV Penetrations)**		
			30%	**50%**	**60%**
E_{demand} (MWh)	71.967	70.449	62.380	56.001	53.046
ΔEsaving (MWh), %	----	1.518 (2.1)	9.587 (13.32)	15.96 (22.18)	18.92 (26.29)
E^{P}_{losses}, MWh	1.675	1.667	1.3625	1.2430	1.2051
E^{Q}_{losses}, MVARh	3.350	3.326	2.639	2.4019	2.2950
Δ E^{P}_{losses} , kWh (%)	---	8 (-.3)	312.5 (18.7)	432 (25.79)	470 (28.05)
ΔE^{Q}_{losses}, KVARh, (%)	------	24 (0.716)	711 (21.22)	948.1 (28.32)	1055 (31.5)

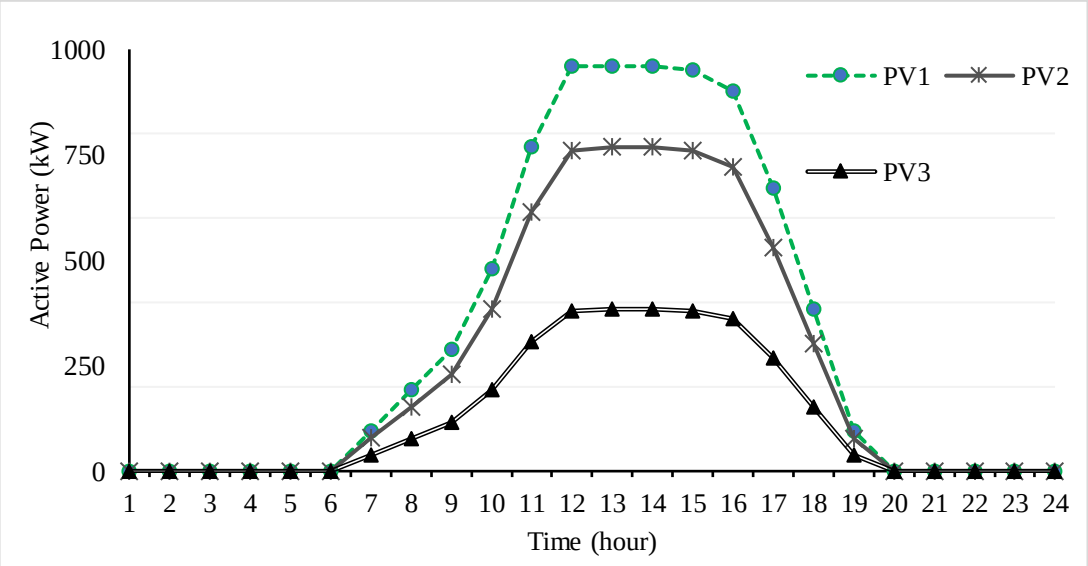

Figure 5.9 Active power profile of PV power systems

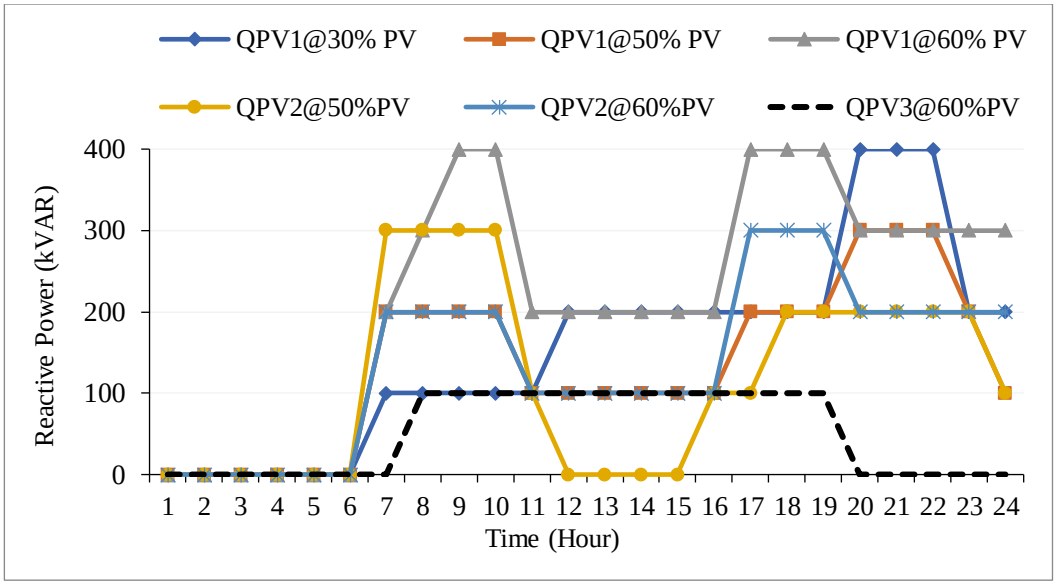

Figure 5.10 Optimal reactive power support from PV inverters

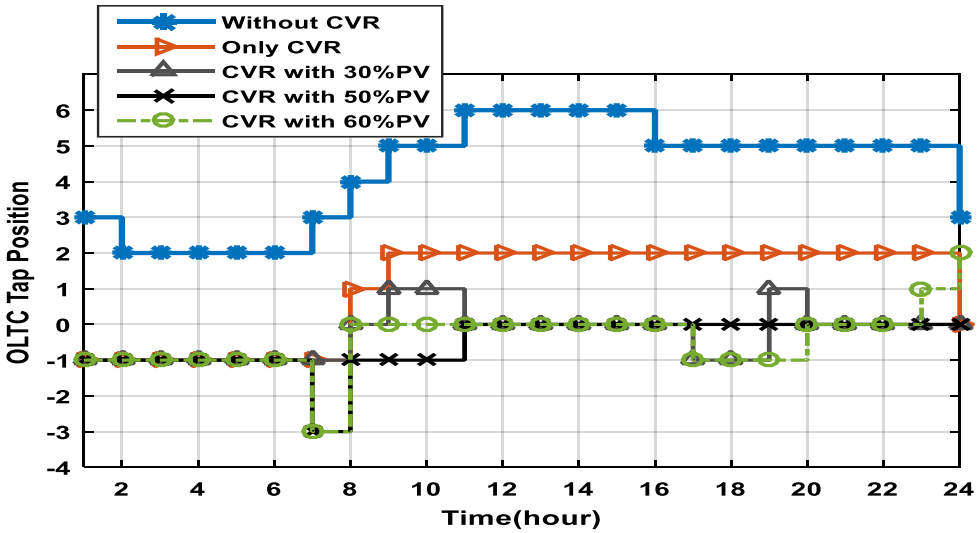

Figure 5.11 OLTC tap position of all modes of operation.

5.5.3.3 Technical and Economical Assessment

The performance of CVR scheme is generally assessed through CVR factor and energy saved. The CVR factors under Mode-2 and Mode-3 operation for both the scenarios has been shown in Figure 5.12. It can be observed from the figure that kW (CVR_{fP}), kWh (CVR_{fE}) and INR (CVR_{fC})) are higher in Mode-3 in comparison to Mode-2. CVR factor in economic terms represents cost savings with respect to voltage reduction.

From Table 5.3, it can be observed that the cost savings achieved is about 2.07 % to 3.31 % with the deployment of CVR in Mode-2 and Mode-3 respectively. While calculating the savings in Mode-3, operational and maintenance cost has been neglected. Table 5.3 presents the reduction in demand cost, loss cost, and total cost also with the enabling of CVR in both Mode-2 and Mode- 3. The reduction in demand cost will directly result in under revenue collection temporarily for a utility point of view. However, this can be rectified later with suitable regulatory schemes such as revenue decoupling mechanism which recovers revenue shortfall including any inevitable interest.

Table 5.3 Demand cost,Loss cost and Total cost saving

Mode		**Demand Cost (kINR)**	**Loss Cost (kINR)**	**Total Cost (kINR)**	**Cost Saving in**		
					kINR	**$***	**%**
Mode-1		215.39	5.148	220.543	-----	---	--
Mode-2		210.85	5.127	215.98	4.53	69.7	2.07
Mode-3	**30%PV**	191.85	4.374	196.228	5.46	84	2.69
	50%PV	176.53	4.086	180.622	5.98	92	3.21
	60%PV	169.44	3.998	173.439	5.93	91.2	3.31

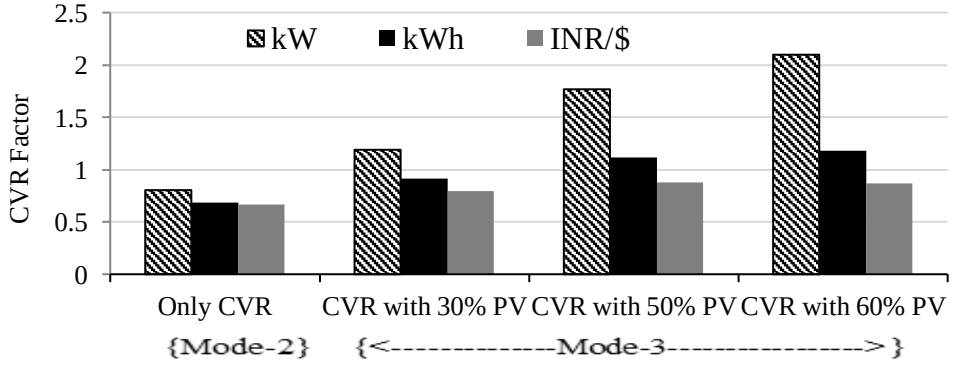

Figure 5.12 CVR factors in terms kW, kWh, INR/$ under Mode-2, and Mode-3

5.5.4 Illustration of Second Stage (FTSC): Local Voltage Control

In order to analyze the effect of fast time scale control, under CVR with 60% PV penetration has been studied. An arbitrary instantaneous point between time intervals from 15:00 to 16:00 has been selected. The load demand is 97% of peak demand at this point and forecasted solar irradiation is 94% of the peak. During this time span, the lowest voltage profile at node 114a becomes vulnerable to any reduction in kW power. Status of Volt/VAR regulation devices OLTC, AVRs, and CBs remain same as in the first stage determined by *algorithm 1*. The fast time scale control has been applied and illustrated for two cases. The droop parameter used in this study is depicted in Appendix B in Table B.2.

5.5.4.1 Case 1 : Single PV power output reduction

In this case, the droop control scheme has been studied when active power for only one PV (PV1) has been varied. The output of other PV systems (PV2 and PV3) remains unchanged. The resulting variation in voltage profile of node 114a with respect to percentage reduction in PV power output has been shown in Figure 5.13. It can be seen that up to 30% reduction in PV1 power output, the lowest voltage remained within minimum allowable voltage limit. Thereafter, the lowest voltage limit violated as the reduction in PV1 power output increases. In order to mitigate the voltage violation, the droop controlled compensating reactive power support has been provided through PV1 inverter. The variation in reactive power support from PV1 inverter has been shown in Figure 5.13. It can be seen from this figure that up to 30% PV power reduction, the injection of compensated reactive power is zero because of lowest voltage profile is within dead-band range. Afterward, the droop controller injects the desired compensating reactive power to meet the lowest voltage profile within the allowable range even when PV1 active power is fully reduced. The effect on active power losses due to the injection

of reactive power from PV inverter has been shown in Figure 5.14. The figure illustrates that total active power losses have also been slightly reducing with droop control action, though the inverter losses are increasing with the control action of droop controller. It happens due to the regeneration of reactive currents in inverter circuitry. Generally, inverter losses due to reactive power compensation are 1-2% of injected/absorbed power. Moreover, the relation $P_t^{inv} = P_t - P_{t,loss}^{inv}$ shows that inverter losses are accommodated P_t unless the value P_t is not zero or not sufficient. From Figure 5.13, at the point when PV1 power is reduced 100 %, the inverter takes power from the grid to bear the inverter losses. In this condition, a slight increase in total active power losses take place as seen in Figure 5.14.

5.5.4.2 Case 2 : Multiple PVs power output reduction

The mutual interference effect has been studied in this case when simultaneously reduction in active power output from more than one PVs is applied. The droop control scheme has been examined by reducing the active power output of both inverters PV1 and PV2 simultaneously. The minimum allowable voltage profile has been observed up to at 29% reduction in power output from both PVs. Further reduction in output would cause a minimum voltage profile violation. In order to mitigate the further reduction in voltage, the compensated droop controlled reactive power support has been enabled through PV1 inverter only. The resulting effect shown in Figure 5.13 indicates that reactive power from PV1 inverter alone is capable of mitigating the voltage violations. The effect on active power losses due to the injection of reactive power from PV inverter has been shown in Figure 5.15. The figure shows that there is a small reduction in total active power losses with droop control action. However, when the reduction in active power output of both the PVs reached above 89%, the total active power losses have been increased slightly. Further, analyzing a case where the active power output reduction in

all PVs sources takes place. The lowest voltage follows the same pattern as the output of both PV1and PV2 was reduced.

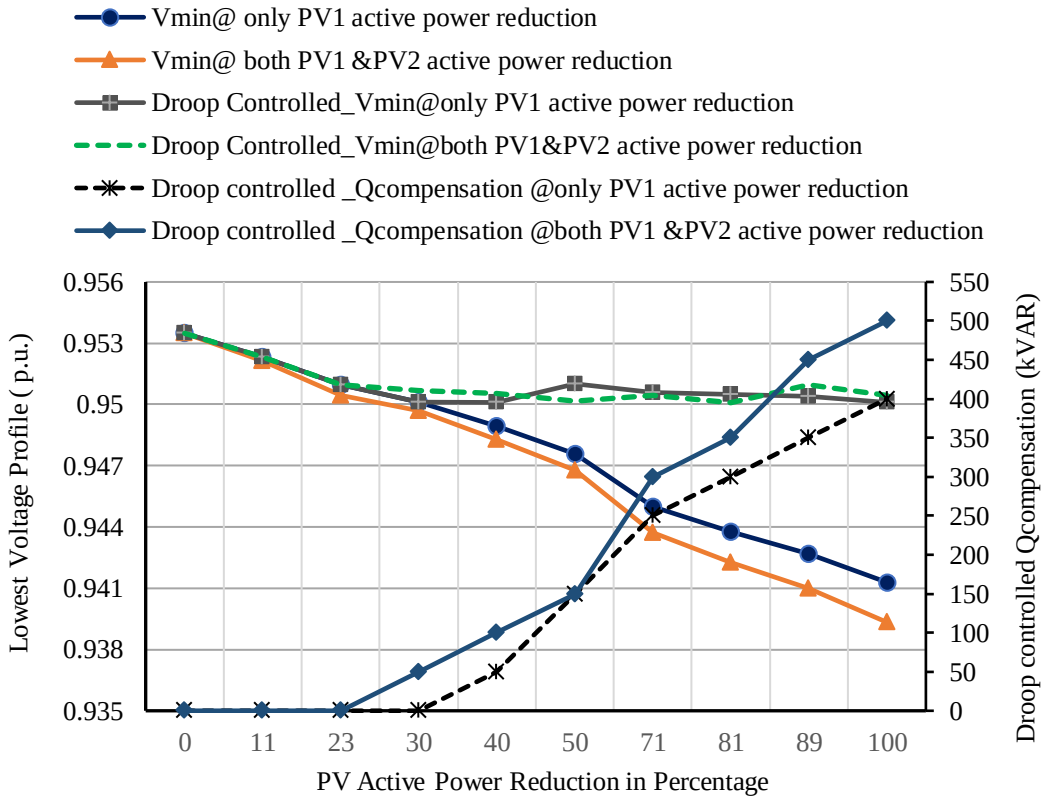

Figure 5.13 Lowest voltage profile at node 114a and compensated Qsupport

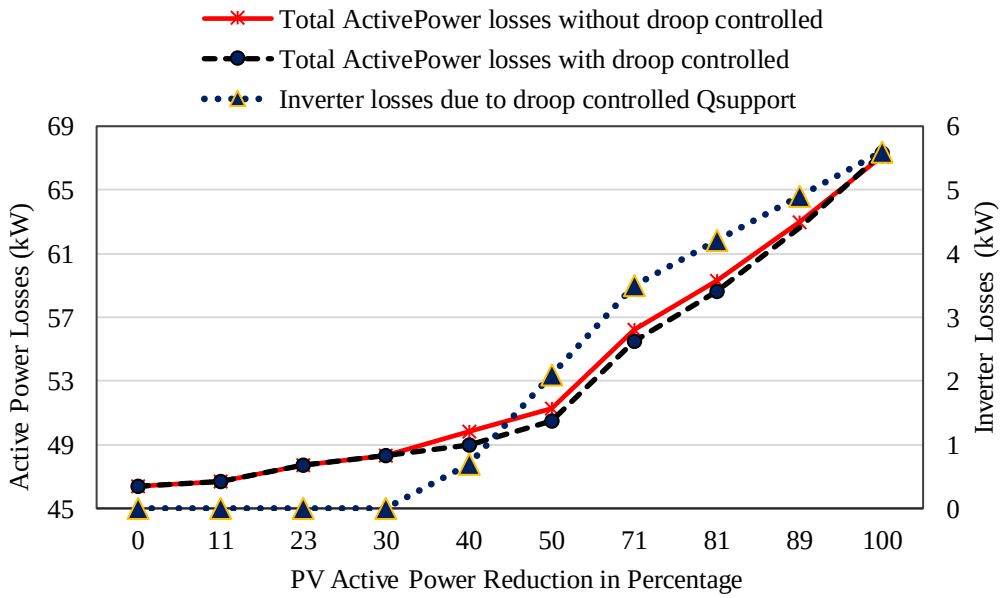

Figure 5.14 Active power losses and inverter losses profile due to PV1 active power reduction.

Considering the condition, where alone PV1 inverter droop controller is not capable of maintaining the voltage profile within the dead-band range. Under such conditions, the local operator may ask to central operators to switch on other PV's droop controllers. While doing so, the coordination among droop controllers would be desired. In case all PV inverters have exhausted compensation limits, the local operator has to ask central operator for compensation from other VVC devices.

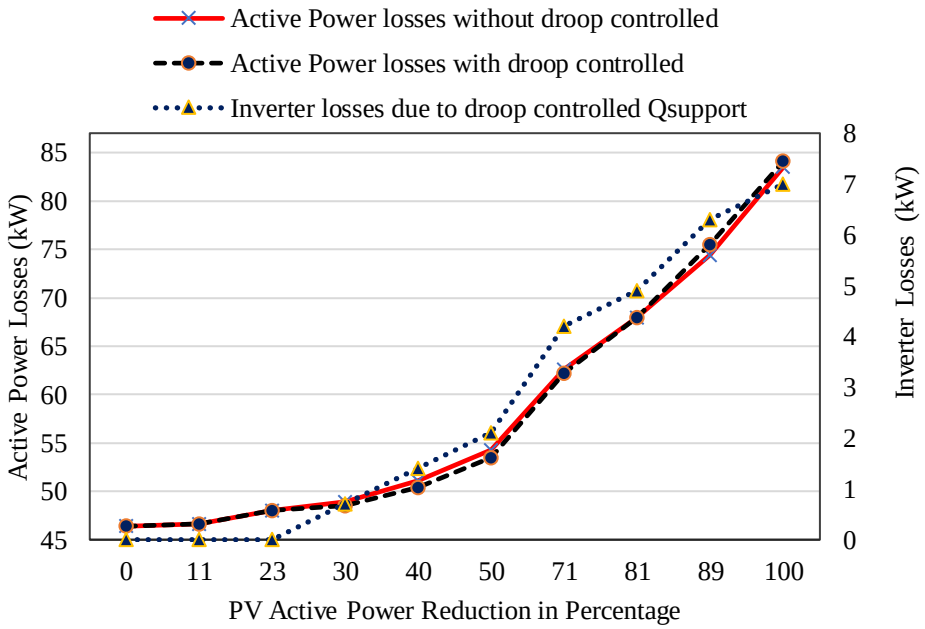

Figure 5.15 Active power losses and inverter losses profile due to PV1and PV2 both active power reduction.

5.5.5 Justification

5.5.5.1 Traditional control Vs Proposed Multi-Stage Control

Implementation of CVR through conventional VVC method has certain limitations regarding voltage reduction range and voltage limit violations during higher demand reduction. The line drop compensation method is widely accepted traditional VVC scheme for CVR deployment. In such studies, the regulated voltages have been is normally fixed at 118V to 120 V and LDC control action is executed in order to enable the CVR operation. The lower voltage limit may violated below the 118V regulated

voltage. Table 5.4 shows the comparative results of Mode -2 operation between traditional and proposed methods. It can be observed that proposed method yields better results in terms of energy demand reduction, loss reduction, and increased CVR factor in comparison to the traditional method with the least variation in lowest voltage profile for a typical day.

5.5.5.2 Centralized Single Stage Control (SSC) Vs Proposed Multi-Stage Control

In centralized SSC, the operation is executed by the control center operator for a fixed time interval ranging from hours to minutes. The settings of VVC devices are tuned according to the defined period.

Table 5.4 Simulation Results in Traditional Method and Proposed Method

Energy Terms	**Mode-1 No-CVR**	**Mode-2 (CVR only)**		**Mode-3 (CVR with PV)**	
		With Traditional Method	**With Proposed Method**	**With Traditional Method**	**With Proposed Method**
Edemand (MWh)	71.967	70.860	70.449	70.860	53.046
∆Esaving (MWh), (%)	---	+1.107 (+1.51)	+1.518 (+2.1)	+1.107 (+1.51)	18.92 (+26.29)
Elosses, MWh	1.675	1.680	1.667	1.680	1.205
∆Elosses, KWh, (%)	---	05 (0.29)	08 (-.3)	05 (0.29)	470 (28.05)
CVR factor (kWh)		0.502	0.642	0.502	1.175
Lowest voltage variations in %	1.1461	1.7025	0.9375	1.7025	1.04

The SSC lacks cooperation when the sudden change in network and intermittent behavior of the PV power output takes place. In that duration, there is a chance of violation in voltage limits. Therefore, the voltage violation ratio remains high. If the optimization and control duration is reduced, say below one hour or 15 minutes, the large data from smart meters and monitoring devices will increase the computational burden. Apart from that, there is a possibility of mishandling or false operations. Moreover, frequent variations in taps of OLTC, AVRs, and switching of CBs will degrade the life cycle of the devices. In order to overcome these issues, the proposed method operates in multi-stages with different time scales. In the first stage, as centralized controlling has been done with the duration of one hour that produces the optimal settings of VVC devices. Moreover, the second stage deals with local control action using a fast response droop controlled based PV inverter in order to handle the voltage fluctuation when any sudden variations in PV power output take place. In conclusion, it can be said that proposed method is beneficial for controlling the operation in centralized as well as in local domains with the less computational burden.

5.6 Conclusion

This chapter has investigated the combined impact of CVR and PV with time-scaled control in various levels of voltage reduction and PV penetrations in the smart grid environment. A discrete multi-objective PSO technique has been used to obtain the optimal setting of controllers. Droop control method has been utilized for fast time scale control to mitigate the voltage drop issue during a sudden fall in PVs active power. The energy and cost savings have been estimated through the proposed method. The findings of this chapter are as under:

- Significant reduction in peak load demand, system losses and daily energy demand have been achieved with only CVR.

- The higher energy and peak savings have been achieved with the deployment of CVR and PV systems. The combined operation of CVR and PV does not result in voltage rise or drop issues even in higher PV penetrations and deeper voltage reduction.
- The economic aspect of CVR deployment has also been analyzed

Thus, it can be concluded that the enabling of CVR control using proposed MSMO-VVC maximizes the CVR benefits in terms of increased voltage reduction range, higher energy and cost savings. In addition, CVR with PV is more beneficial in comparison to CVR or PV alone. Though the proposed methodology works well for CVR implementation, it lacks under transient conditions and presence of intermittency in PV power generations and loads. Hence, there is a need for inclusion of uncertainties (in power generation and loads) impact in VVO model. Moreover, modern ADN demands also fast changing due to the inclusion of flexible loads such as EVs. In this context, next *chapter 6*, analyze EV and uncertainty impact in VVO formulations through model predictive approach.